Measurement of rotation- and strain- rate tensors by using stereoscopic PIV

by

O. Özcan[(1)] , K.E. Meyer[(2)] and P.S. Larsen[(2)]

[(1)] Yildiz Technical University, Dept. of Mechanical Eng., 34349, Istanbul, Turkey

[(1)] E-Mail: oktayo@yildiz.edu.tr

[(2)] Technical University of Denmark, Dept. of Mechanical Eng., Building 403, DK-2800,Lyngby, Denmark

[(2)]E-Mail: kem@mek.dtu.dk, psl@mek.dtu.dk

ABSTRACT

A simple technique is described for measuring the mean rate−of−displacement (velocity gradient) tensor in a plane by using a conventional stereoscopic PIV system. The technique involves taking PIV data in two or three closely−spaced parallel planes at different times. All components of the mean rate–of–displacement tensor are then calculated by using finite difference formulas. Planar measurements of the mean vorticity vector, rate−of−rotation and rate−of−strain tensors and the production of turbulent kinetic energy can be accomplished. Parameters of the Q–criterion and negative–λ_2 techniques used for vortex identification can be evaluated in the mean flow field. Dissipation rate of the turbulent kinetic energy in a non−isotropic three−dimensional flow field may also be estimated. Experimental data obtained for a round turbulent jet normal to a crossflow in a low−speed wind tunnel are presented to show the applicability of the proposed technique. The PIV cameras and light sheet optics shown in Fig. 1a are mounted on the same traverse mechanism in order to displace the measurement plane accurately. Data obtained in constant–y and –z planes are presented. Fig. 1b shows a contour plot of the normalized production rate of turbulent kinetic energy $P^*=PD/U^3$ in the z/D=2 plane (D is the jet diameter, U is the crossflow velocity). P^* is evaluated by using its exact definition, i.e., all nine additive terms in the definition are included. Smoothness of the contour plot indicates the successful implementation of the technique. Measurement uncertainties are discussed and algebraic relations for uncertainties in P and the parameter of the Q–criterion are presented. Consistency of the measurements is verified by showing agreement of two data sets obtained in two perpendicular planes. Accuracy of the data can be improved if optimal spacing between velocity vectors is employed. The feasibility of measuring the truncation error in the rotation– and strain–rate tensors is also demonstrated.

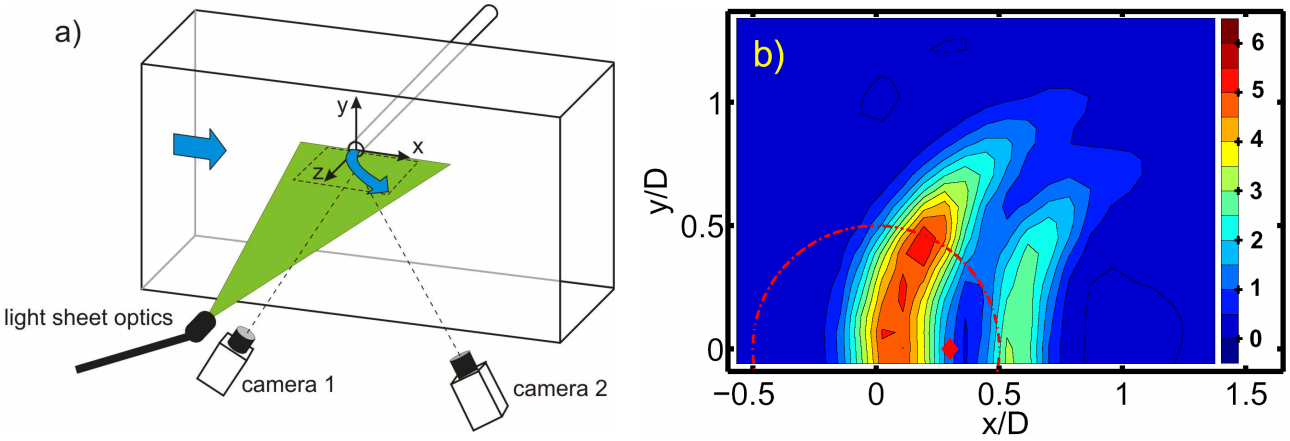

Fig. 1 a) Schematic description of experimental set–up, b) Contour plot of the normalized production rate of turbulent kinetic energy $P^*=PD/U^3$ in the z/D=2 plane , Uncertainty in P^* is 0.25 (Red dashed line and diamond symbol indicate the jet exit and the location of the jet trajectory, respectively).

1. INTRODUCTION

The rate−of−displacement tensor is an important quantity in the analysis of problems in Fluid Mechanics. A knowledge of the decomposition into rotation− and strain−rate tensors is necessary for modeling turbulence, validating constitutive relations, identifying vortices and understanding the physical structure of a flow. However, measurement of the rate−of−displacement tensor is a challenging task which requires acquisition of all three components of the velocity vector at a number of points that are slightly displaced along three mutually perpendicular directions. Wallace and Foss (1995) describe the difficulties in measuring the rate−of−rotation tensor in turbulent flows. The hot−wire anemometry and the Laser Doppler Anemometry (LDA) are in principle capable of measuring the rate−of−displacement tensor at a point. Andreopoulos and Honkan (1996) and Zhou et al.(2003) describe hot−wire probes (consisting of 9 and 8 wires, respectively) capable of measuring the instantaneous rate−of−displacement tensor. However, long data acquisition times may render the point–based measurement techniques impractical. The holographic PIV (Particle Image Velocimetry) technique (Meng and Hussain, 1993, Tao, 2000), which measures all three components of the velocity vector in a volume, readily produces the rate−of−displacement tensor. However, holographic PIV is a relatively new technique based on photographic recording, which requires long data processing times and large computer memory that severely limit the number of realizations used in data averaging. The scalar imaging velocimetry (Dahm et al., 1992) and the three−dimensional particle tracking velocimetry (Nishino et al., 1989) also produce all components of the instantaneous rate−of−displacement tensor in a volume. The latter technique generally provides poor spatial resolution wheras the former is applicable to high Schmidt number flows. The dual plane PIV (Hu et al., 2001, Mullin and Dahm, 2003) is probably the best technique available today for measuring the instantaneous rate−of−displacement tensor. However, the dual plane PIV has a high cost and additional alignment requirements since it is basically equivalent to two stereoscopic PIV systems used in tandem.

The present paper describes a simple technique for measuring the mean rate–of–displacement tensor in a plane by using a conventional stereoscopic PIV system that records all three components of the instantaneous velocity vector. The technique involves taking PIV data in two or three closely−spaced parallel planes at different times and is applicable to a broad range of flows (compressible, incompressible, steady, unsteady, laminar, turbulent). All components of the mean rate−of−displacement tensor are calculated by using finite differences. Planar measurements of the mean vorticity vector, rotation− and strain−rate tensors and the production of turbulent kinetic energy can be readily accomplished. Dissipation rate of the turbulent kinetic energy can also be estimated if the interrogation area size is sufficiently small in a general, non–isotropic three–dimensional flow. In general, the method requires large samples and good spatial resolution. Experimental data obtained for a jet in crossflow are presented to show the applicability of the proposed technique. The test flow, which is highly turbulent, vortical and three−dimensional, involves flow reversals in all three directions and can be best studied by a directionally sensitive non−intrusive technique. Data averaged over a thousand vector maps along the intersection of two perpendicular planes are compared with each other to assess the consistency of the technique. Some earlier results on the successful implementation of the technique was presented in Meyer et al. (2001) which reported that the deviator of the rate–of–displacement tensor is not aligned with the deviatoric Reynolds stress (i.e., the gradient–transport approximation is not valid) for a jet in crossflow.

2. RATE–OF–DISPLACEMENT TENSOR

The mean rate−of−displacement tensor d_{ij} is defined by

$$d_{ij} = \partial u_i / \partial x_j \tag{1}$$

where u_i are the mean velocity components and x_j are the space variables in a Cartesian coordinate system, i and j (=1,2,3) being free indices. d_{ij} can be decomposed into the summation of the symmetrical rate−of−strain (deformation) tensor s_{ij} and the skew−symmetrical rate−of−rotation (spin) tensor r_{ij} which are given by (Tennekes and Lumley, 1972)

$$s_{ij} = (\partial u_i / \partial x_j + \partial u_j / \partial x_i) / 2 \tag{2}$$

$$r_{ij} = (\partial u_i / \partial x_j - \partial u_j / \partial x_i) / 2 \tag{3}$$

The mean vorticity vector ζ_i, which is twice the angular velocity vector, is related to the rate−of−rotation tensor by

$$\zeta_i = e_{ijm}\, r_{mj} \tag{4}$$

where e_{ijm} is the permutation symbol. A repeated index implies summation unless indicated otherwise. The strain−rate tensor s_{ij} can be written as the summation of deviatoric and isotropic tensors which are measures of the rate−of−distortion and the rate−of−dilatation (volumetric expansion), respectively. The rates of production and viscous dissipation of turbulent kinetic energy (P and ε), which are important parameters in most models of turbulence, are related to the mean and fluctuating rate−of−strain tensors s_{ij} and s'_{ij}, respectively by (Tennekes and Lumley, 1972)

$$P = - \langle u'_i\, u'_j \rangle\, s_{ij} \tag{5}$$

$$\varepsilon = 2\nu \langle s'_{ij}\, s'_{ij} \rangle \tag{6}$$

where brackets $\langle\ \rangle$ denote averaging, ν is the kinematic viscosity, u'_i is the fluctuating velocity vector and $\langle u'_i\, u'_j \rangle$ is the Reynolds stress tensor (divided by density). The fluctuating deformation rate tensor s'_{ij} is defined by an equation similar to Eq. (2) where u_i is replaced by u'_i. The Q−criterion technique used in vortex identification evaluates the following scalar (Hunt et al., 1988)

$$Q = (r_{ij}\, r_{ij} - s_{ij}\, s_{ij}) / 2 \tag{7}$$

which is the second invariant of the mean rate−of−displacement tensor. Jeong and Hussain (1995) report that the second largest eigenvalue of $(s_{ik}\, s_{kj} + r_{ik}\, r_{kj})$, which is named λ_2, is generally a better parameter than Q in identifying a vortex. High positive values of Q and negative values of λ_2 identify vortical flow regions where the rotation rate dominates the strain rate in the mean flow field.

3. EXPERIMENTAL METHOD AND SET−UP

The proposed technique involves acquisition of sterescopic PIV data in two or three closely−spaced parallel planes at different times. A conventional stereoscopic PIV system measures all three components of the instantaneous velocity vector in a plane. Averaging of PIV vector maps produces all three components of the mean velocity and six components of the Reynolds stress tensor. In−plane−gradients of all velocity components can be calculated by using the central difference scheme which is accurate to second order. The gradients of all mean velocity components in the out−of−plane direction can be evaluated by using the forward difference scheme which is accurate to first order when PIV data is obtained in only two closely−spaced parallel planes. Accuracy of the velocity gradients in the out−of−plane direction can be improved by taking data in three closely−spaced parallel planes and employing the central difference scheme. Once d_{ij} is known, s_{ij}, r_{ij}, ζ_i, P and Q can be calculated from Eqns. (2), (3), (4), (5) and (7), respectively. Components of the fluctuating rate−of−deformation tensor involving in−plane−gradients of three fluctuating velocity components can be calculated in a similar manner. However, since data in parallel planes are not obtained simultaneously, the three out−of−plane derivatives of the fluctuating velocity components cannot be measured. Yet, one of these can be derived from a knowledge of two in−plane−gradients of the fluctuating velocity field which is divergence free for incompressible flow. By neglecting the remaining two out−of−plane gradients in Eq. (6), one can obtain an estimate of the turbulent dissipation rate for a general (non−isotropic) three−dimensional flow. (The estimate could potentially be improved by simply using *9/7* times the *7* recorded contributions on account of the approach to isotropy of small scales.) An accurate measurement of the dissipation rate of the turbulent kinetic energy requires a rather small interrogation area size and small separation distance between the parallel laser planes (both smaller than a few Kolmogorov viscous length scales) as will be discussed later.

The rate−of−displacement tensor was measured in the flow field of a turbulent non−buoyant jet in crossflow in a low speed wind tunnel with test section dimensions of 300 by 600 *mm* at the Technical University of Denmark. Fig.1a gives a schematic description of the experimental set−up. The jet issued normal to a flat plate insert through a circular pipe of diameter D = 24 *mm* with a bulk velocity of W = 4.95 *m/s*. The crossflow velocity along the flat plate was U = 1.50 *m/s*, producing a jet−to−crossflow velocity ratio *W/U* of 3.3. The Reynolds number based on the jet diameter D and the crossflow velocity U was 2400 nominally. Special consideration was given to establish fully−developed and self−preserved incoming flows in the pipe and on the flat plate, respectively. The results are discussed in reference to the (*x,y,z*) Cartesian coordinate system whose origin is at the center of the pipe at the jet exit as shown in Fig.1a. More

information on the flow conditions can be found in Meyer et al. (2001), Meyer et al. (2002) and Özcan and Larsen (2003) who reported some early findings. Pedersen (2003) studied the coherent structures in the flow field by using the POD (Proper Orthogonal Decomposition) analysis.

The PIV system shown in Fig.1a consisted of two Kodak Megaplus ES 1.0 cameras with 60 *mm* Nikon lenses mounted in near−Scheimpflug condition (angle between the cameras was 80°). A double cavity Nd−YAG laser delivering 100 *mJ* light pulses was employed to create a light sheet which was 1.5 *mm* thick. Cameras and light sheet optics were mounted on the same traverse mechanism in order to accurately displace the measurement plane. Both the crossflow and the jet flow were seeded with 2−3 μm droplets of glycerol. The system was controlled by a Dantec PIV2100 processor and the data were processed with Dantec Flowmanager version 3.4 using adaptive velocity correlation. 25 percent overlap was used between interrogation areas. A calibration target aligned with the light sheet plane was used to obtain the geometrical information required for the reconstruction of the velocity vectors. The reconstruction was performed by using a linear transformation and the calibration images were recorded for five slightly−displaced planes. Image maps were recorded with an acquisition rate of 0.5 *Hz* to yield 1000 instantaneous vector maps used to calculate the velocity moments. Two different configurations of the cameras and the light sheet were used to obtain data in constant−y (as shown in Fig.1a) and constant−z planes, having fields of view of 108 by 86 *mm* and 65 by 53 *mm*, respectively. In both cases the velocity vector maps contained 33 by 37 vectors. Therefore, the linear dimensions of the interrogation areas varied between 1.5 and 3.4 *mm*. The rate of displacement tensor data to be presented are obtained at the z= 48 *mm* and 50 *mm* planes and also at the y=24 *mm* and 27 *mm* planes. Thus, results are presented for the z=49 *mm* and y=25.5 *mm* planes which are nominally referred to as z/D=2 and y/D=1 planes.

4. MEASUREMENT UNCERTAINTIES

Table 1 presents the values of the spacing between velocity vectors δx, δy and δz for the data of z/D=2 and y/D=1 planes together with the estimated uncertainties in the normalized quantities at the intersection of the two planes. Uncertainties of the quantities to be presented in contour plots are stated in figure captions. Δq^*, Δk^*, Δd^*_{ij} and ΔP^* are the uncertainties (plus and minus) in the normalized speed, turbulent kinetic energy, the rate−of−displacement (also rotation and strain) tensor components, and the production rate of turbulent kinetic energy, respectively. T^*_{ij} is the truncation error (see below). All uncertainties are specified for a confidence level of 95 percent. The crossflow velocity U and the jet diameter D were used for normalization of the uncertainties. The possible use of the jet velocity W in the normalization would produce smaller uncertainties. Lourenco and Krothapalli (1995) report that the error in the measurement of the rate−of−displacement tensor can be divided into two components. One is the truncation error associated with the finite difference scheme employed and the other is due to uncertainty in the velocity measurement. The velocity measurement error and the truncation error increase and decrease, respectively, as the spacing between the velocity vectors become smaller. Therefore, the total error in the rate−of−displacement tensor is minimal for an optimum spacing between the velocity vectors. Saarentino and Piiorto (2000) suggest that the value of the optimal spacing is 3 to 5 Kolmogorov viscous length scales for PIV measurements. In hot—wire anemometry, the same value of optimal spacing between velocity vectors is chosen as reported by Antonia and Mi (1993) and Zhou et al. (2003). In the flow of the present study, the Kolmogorov length scale is estimated from isotropic turbulence relations as 0.12 *mm* which would make the optimal spacing between velocity vectors approximately 0.5 *mm*. The spacing values shown in Table 1 are 3 to 7 times larger than the optimal value. PIV data of Kawanabe et al. (2001) show that the first and second moments of the velocity (and the production of turbulent kinetic energy) do not vary much with the variations of the interrogation area size whereas the dissipation rate of turbulent kinetic energy increases significantly with increased spatial resolution until the optimal value is reached. Even though the spatial resolution of the experimental data used in the present study is not sufficient for measurement of the dissipation rate, results will be presented to show the applicability of the proposed technique. If the optimal spacing had been used in the present study, the estimated uncertainties Δd^*_{ij} and ΔP^* given in Table 1 could probably be reduced to 0.07 and 0.04, respectively. However, this would cause a reduction in the size of the field of view by a factor of approximately four.

Data Plane	δx *(mm)*	δy *(mm)*	δz *(mm)*	Δq^*	Δk^*	Δd^*_{ij}	ΔP^*	T^*_{ij}
z/D=2	2.0	1.5	2.0	0.07	0.025	0.11	0.07	0.08
y/D=1	2.4	3.0	3.4	0.07	0.025	0.14	0.10	0.12

Table 1- Spacing between velocity vectors and estimated uncertainties in quantities at the intersection of the planes

The truncation error T_{ij} in the rate−of−displacement tensor d_{ij} calculated by the central difference scheme given by

$$T_{ij} = - \left(\partial^3 u_i / \partial x_j^3 \right) \left(\delta x_j \right)^2 / 6 \qquad (8)$$

where the repeated index j does not imply summation. The normalized bound values of T_{ij} are given in Table 1. If third order spatial derivatives of the flow field are known, the truncation error can be estimated from Eq. (8) as discussed in the next section. Since the truncation error is a systematic (bias) error, in principle, it can be removed by applying a correction to the rate−of−displacement tensor d_{ij} . However, measurement of the third order derivatives in the out−of−plane direction requires data acquisition in four slightly−displaced parallel planes.

The uncertainty in the rate of production of turbulent kinetic energy ΔP can be estimated by applying the error propagation formula of Kline and McClintock (Holman,1978) to Eq. (5) which produces

$$\Delta P = \left[s_{ij} \; s_{ij} \; (\Delta A)^2 + \langle u'_i \, u'_j \rangle \langle u'_i \, u'_j \rangle \, (\Delta B)^2 \right]^{1/2} \qquad (9)$$

where ΔA and ΔB are the uncertainties in $\langle u'_i \, u'_j \rangle$ and d_{ij} (or s_{ij} and r_{ij}), respectively, which are assumed to be equal for all components of the tensors. The error analysis of Benedict and Gould (1996) indicates that ΔA can be estimated from

$$\Delta A = 2 \; u_{rms} \, \Delta u_{rms} \qquad (10)$$

where u_{rms} is the root−mean−square of the velocity fluctuations and Δu_{rms} is the uncertainty in u_{rms} which was assumed to be equal in all three directions. The value of Δu_{rms} was chosen as $0.025U$ in estimating the ΔP uncertainty. The uncertainty in the parameter of the Q−criterion may be estimated from

$$\Delta Q = \left[8 \, r_{ij} \; r_{ij} + 4 \, (s_{ii})^2 + 8 (s_{ij} \; s_{ij} - s_{ii}^2) \right]^{1/2} \; \Delta B \qquad (11)$$

5. RESULTS AND DISCUSSION

Figs. 1b , 2a and 2b present contour plots of the normalized production rate of turbulent kinetic energy $P^* = PD/U^3$, the normalized vorticity magnitude $\omega^* = 2(r^2_{zy} + r^2_{xz} + r^2_{yx})^{1/2} \, D/U$, and the normalized value of Q parameter $Q^* = QD^2/U^2$, respectively, in the z/D=2 plane. The aim here is not to emphasize the flow physics but rather to demonstrate the performance of the proposed technique. The thin and thick dashed−lines indicate the jet exit and the zero value contours, respectively, in these and all subsequent figures. The filled−diamond symbol at y/D=0 (line and plane of symmetry) and x/D=0.3 denotes intersection of jet trajectory with the z/D=2 plane. Smoothness of the contours is indicative of good data quality. The largest component of vorticity (in absolute value) in this plane is $\zeta_y = 2r_{yx}$ which is negative upstream of the jet trajectory and positive downstream of it due to the action of the jet shear layer vortices. The kidney−shaped contours of the vorticity magnitude around the jet exit are similar to those of ζ_y. Fig.1b shows that production of turbulent kinetic energy is significantly large around the jet exit. The vortical structures at the jet exit (the jet shear layer vortices and the counter−rotating vortex pair, Lim et al., 2001) stretch the flow field and cause an energy transfer from the mean field to turbulence which generates turbulent kinetic energy values that are significantly larger than those of the incoming jet and crossflow. Comparison of Figs. 1b and 2a shows that P^* contours are similar to those of the vorticity magnitude around the jet trajectory but the production rate of

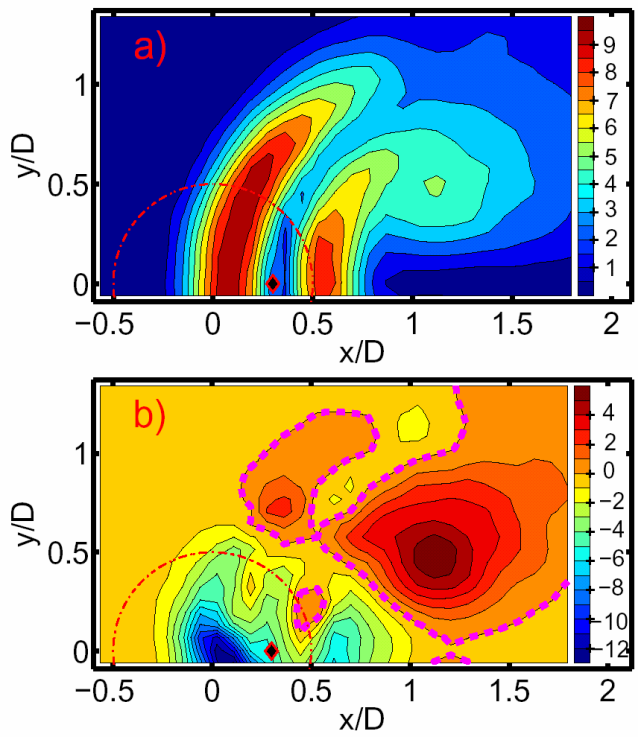

Fig. 2 Contour plots of a) the normalized vorticity magnitude $\omega^* = 2\,(r^2_{zy} + r^2_{xz} + r^2_{yx})^{1/2}\,D/U$, *b) the normalized value of the Q parameter* $Q^* = QD^2/U^2$ *in the z/D=2 plane. Uncertainties in* ω^* *and* Q^* *are 0.4 and 1.5, respectively.*

turbulent kinetic energy diminishes much faster than the vorticity magnitude away from the jet trajectory where the Reynolds stresses are small. Fig. 2b shows that the maximal positive values of Q^* are located around points A (x/D=1.1, y/D=0.5) and B (x/D=0.4, y/D=0.7). These locations correspond very closely to the positive and negative z-vorticity regions, respectively, which are caused by the side arms of the upstream and lee-side vortex loops in the vortex skeleton model of Lim et al (2001). Fig. 2a shows that the maximal value locations of the vorticity magnitude are not related to points A and B which are the presumed vortex cores in this plane. This is a well-known inadequacy of the vorticity magnitude in identifying vortex cores (Jeong and Hussain, 1995).

Figs. 3a and 3b present contour plots of the normalized second largest eigenvalue of $(s_{ik}s_{kj} + r_{ik}r_{kj})$, $\lambda_2^* = \lambda_2 D^2/U^2$ and the normalized summation of eigenvalues (of $s_{ik}s_{kj} + r_{ik}r_{kj}$), $\lambda_{SUM}^* = (\lambda_1 + \lambda_2 + \lambda_3)D^2/U^2$ in the z/D=2 plane, respectively. Jeong and Hussain (1995) report that negative values of λ_2 indicate a vortex core. Comparison of Figs. 3a and 2b shows that positive Q and negative λ_2 criteria are almost equivalent in this plane. Contours in Figs. 3b and 2b are identical due to the fact that $\lambda_{SUM}^* = -2Q^*$ (Jeong and Hussain ,1995). This result shows that accuracy of the eigenvalue determination is satisfactorily high.

Fig. 4a presents contour plots of the normalized third order spatial derivative $(\partial^3 u / \partial x^3)D^3/U$ in the z/D=2 plane. The thick dashed lines indicate zero value contours. The central difference scheme was used to evaluate the derivative. Smoothness of the contours suggest that measurement of the first and second spatial derivatives of the mean rate-of-displacement tensor may be accomplished with reasonable accuracy. A knowledge of these derivatives may be useful in modeling turbulence and estimating the truncation error (given by Eq.(8)) in the rate-of-displacement tensor. $\partial^3 u/\partial x^3$ changes sign at least three times along the x direction when y/D is smaller than one. Fig. 4b shows variations of the normalized truncation error of $T_{ij}D/U$ predicted by Eq. (8) at the intersection of the y/D=1 and z/D=2 planes. T_{xy}, T_{yy} and T_{zy} were evaluated by using the data of the y/D=1 plane whereas the remaining T_{ij} components were calculated from the z/D=2 plane data. All of T_{ij} values are smaller than the estimated error bounds given in Table 1.

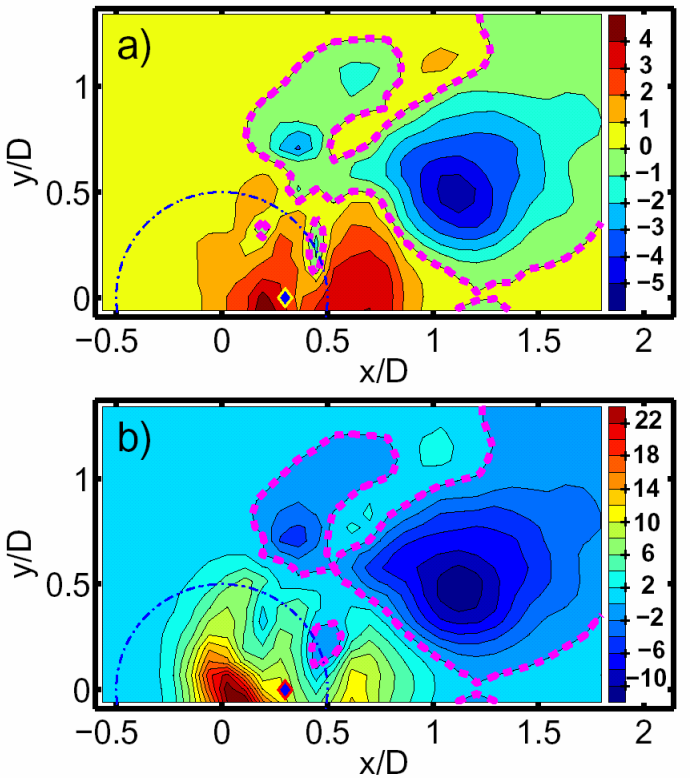

Fig. 3 Contour plots of a) the normalized value of the second largest eigenvalue (of $s_{ik}s_{kj} + r_{ik}r_{kj}$) $\lambda_2^* = \lambda_2 D^2/U^2$ b) the normalized value of the summation of eigenvalues $\lambda_{SUM}^* = (\lambda_1 + \lambda_2 + \lambda_3)D^2/U^2$ in the z/D=2 plane. Uncertainties in λ_2^* and λ_{SUM}^* are 0.9 and 1.5, respectively.

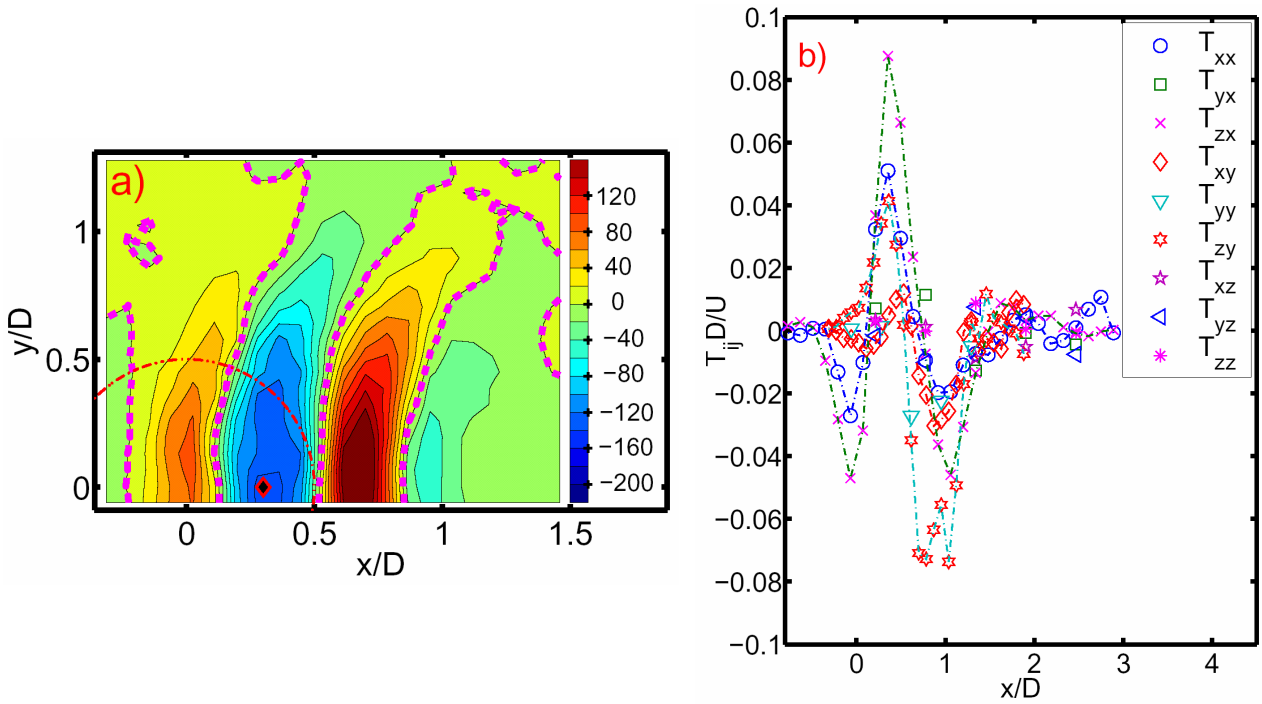

Fig. 4 a) Contour plot of the normalized third order spatial derivative $(\partial^3 u / \partial x^3)D^3/U$ in the z/D=2 plane. b) Variation of the normalized truncation error T_{ij}^* at the intersection of the y/D=1 and z/D=2 planes.

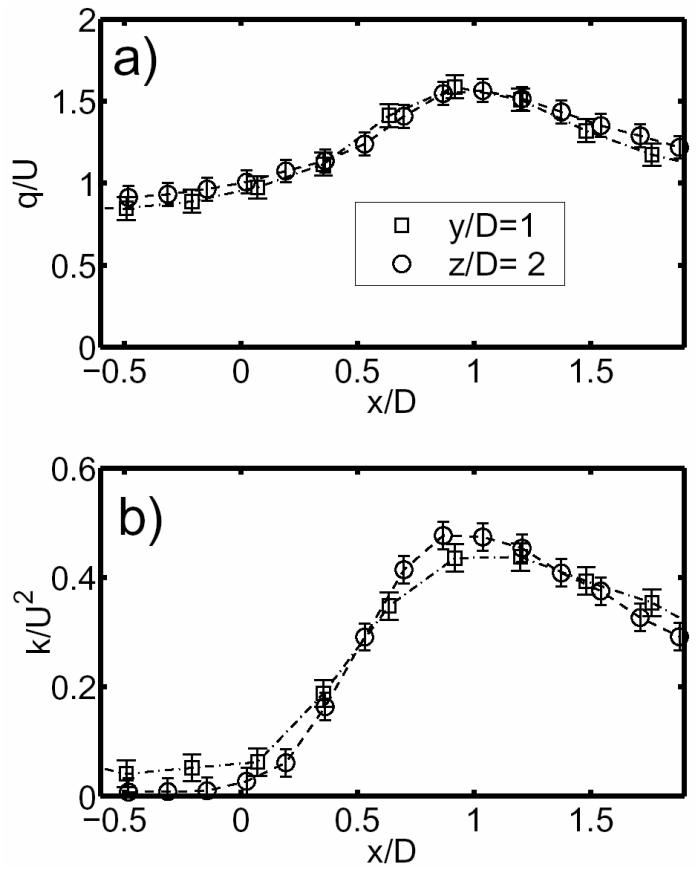

Fig. 5 Variations of a) the normalized speed $q^* = q/U$, b) the normalized turbulent kinetic energy $k^* = k/U^2$ at the intersection of the y/D=1 and z/D=2 planes.

In the remaining section of the paper, variation of the data obtained in the y/D=1 and z/D=2 planes along the intersection line of the planes will be compared with each other in order to assess the consistency of the measurements. A good agreement of the first and second moments of the velocity between the two data sets is necessary if one further expects to see an agreement of the rate-of-displacement tensor components. Figs. 5a and 5b give variations of the normalized speed $q^* = q/U = (u_i\, u_i)^{1/2}/U$ and the normalized turbulent kinetic energy $k^* = k/U^2 = < u'_i\, u'_i >/2U^2$, respectively, with x/D. The legend shows the plane of the two data sets. Uncertainty in the data is indicated by error bars in this and all subsequent figures. As the higher momentum jet traverses across the crossflow , the mean speed first increases and then decreases with increasing x/D. A similar trend of the turbulent kinetic energy is also observed since the production of turbulent kinetic energy is maximal around the jet trajectory as shown in Fig.1b. Fig. 5 shows that the differences between the two data sets are smaller than the measurement uncertainties. This indicates that repeatability of the experiment was sufficiently good.

Figs. 6a, 6b and 6c give variations of the normalized components of the rate-of-rotation tensor r^*_{yx}, r^*_{xz} and r^*_{zy} ($r^*_{ij} = r_{ij} D/U$), respectively, with x/D for data obtained in the y/D=1 and z/D=2 planes. These components are equal to one-half of the vorticity vector components in the z, y and x directions. Fig. 6 shows that r^*_{zy} is always negative whereas r^*_{yx} and r^*_{xz} change sign more than once in this region of the flow. A negative value of r^*_{zy} is ssociated with rotation in the clockwise direction in constant-x planes when looking in the negative x direction.. Fig. 6c shows that the CVP, which rotates in the clockwise direction begins to form at a surprisingly small x/D value of 0.1. Negative and positive values of r^*_{xz} are associated with rotation in the counter-clockwise and clockwise directions in constant-y planes when looking in the positive y direction. Fig. 6b shows that r^*_{xz} changes sign from negative to positive around x=1 which may be interpreted as the boundary between the counter-clockwise and

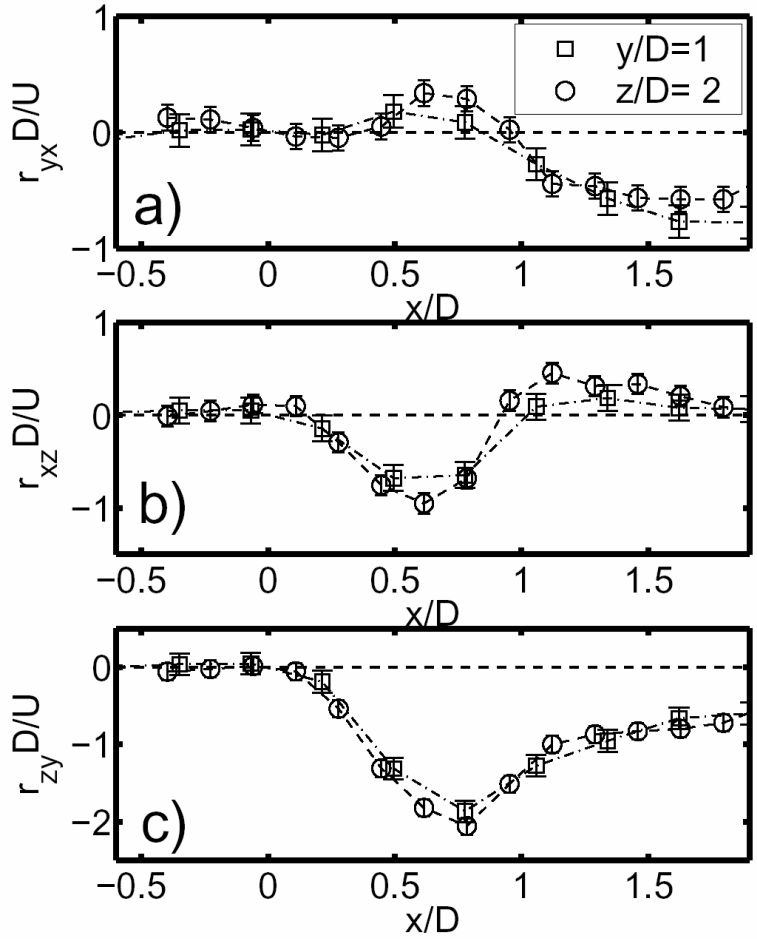

Fig. 6 Variations of the normalized components of the rate−of−rotation tensor a) r^*_{yx}, b) r^*_{xz}, c) r^*_{zy} at the intersection of the y/D=1 and z/D=2 planes.

clockwise rotating jet shear layer vortices (i.e., the upstream vortex loops and lee−side vortex loops in the vortex skeleton model of Lim et al. (2001)). Negative and positive values of r^*_{yx} are due to clockwise and counter−clockwise rotating vortices in constant−z planes when looking in the negative z direction.. These vortices are probably the side arms of the lee−side and upstream vortex loops.

Figs. 7a, 7b and 7c present variations of the normalized components of the rate−of−strain tensor s^*_{yx}, s^*_{xz} and s^*_{zy} ($s^*_{ij} = s_{ij} D/U$), respectively, with x/D for data obtained in the y/D=1 and z/D=2 planes. s^*_{yx}, s^*_{xz} and s^*_{zy} are measures of the rate of distortion in the constant z, y and x planes for the incompressible flow field considered in the present study. Similar to the rate−of−rotation tensor components, s^*_{zy} is always negative whereas s^*_{yx} and s^*_{xz} change sign more than once. The magnitude of the rate−of−strain tensor components are smaller than those of the rate−of−rotation tensor which indicates that rotation is larger than distortion generally. Relatively large values of s^*_{zy} shown in Fig. 7c indicates that there is significant deformation mainly in the x direction around the jet exit.

Figs. 8a and 8b present variations of the normalized production and dissipation of turbulent kinetic energy ($P^* = PD/U^3$ and $\varepsilon^* = \varepsilon D/U^3$), respectively, with x/D for the data obtained in the y/D=1 and z/D=2 planes. Both the production and the dissipation rates, which are negligibly small for negative values of x/D, reach maximal values around x/D=0.8 and decrease monotonically for larger values of x/D. The rate of production decreases much more rapidly than the rate of dissipation. This result suggests that turbulent kinetic energy producing coherent structures coexist with highly dissipative small scale eddies around the jet core. Outside the jet core, the production process stops abruptly whereas the dissipation process continues at a lower rate. No error bars are shown for ε^* which have unknown accuracy as discussed earlier. Fig. 8b shows that, as expected, dissipation rate values for the z/D=2 plane data are significantly larger than those for the y/D=1 plane, which have lower spatial resolution. The same trend is seen in Fig. 8a although to a lesser degree.

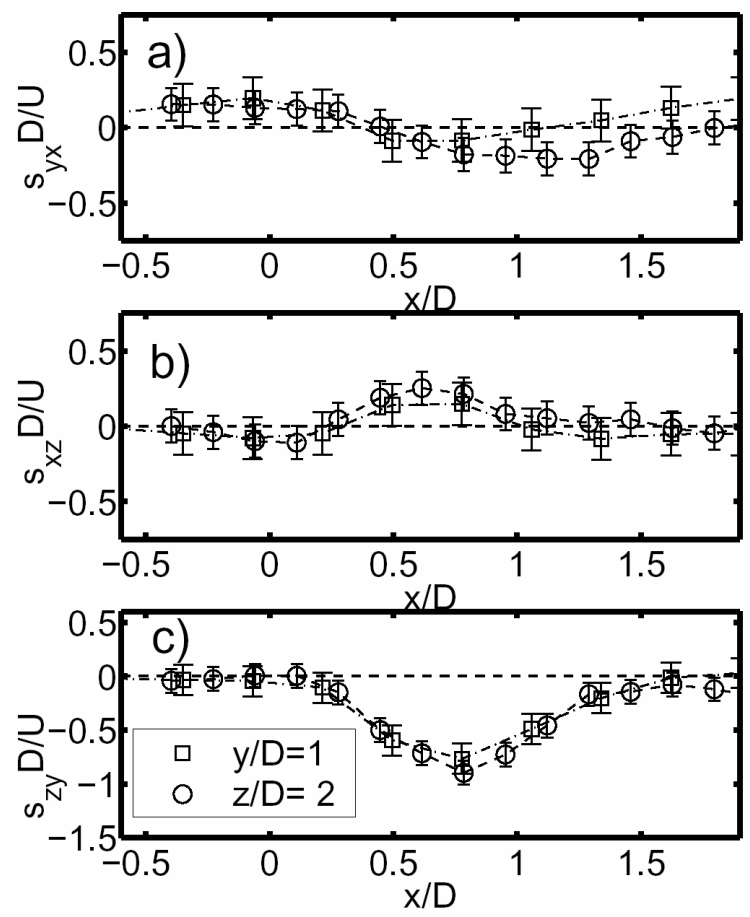

Fig. 7 Variations of the normalized components of the rate−of−strain tensor a) s^*_{yx}, b) s^*_{xz}, c) s^*_{zy} at the intersection of the y/D=1 and z/D=2 planes.

Figs. 6, 7 and 8 show that the data sets obtained in the *y/D*=1 and *z/D*=2 planes agree with each other within the measurement uncertainties. This agreement indicates consistency of the measurements. The magnitude of the error bars in Figs. 6 to 8 is considerably large compared to the values of r^*_{ij}, s^*_{ij} and P^*, which are low in this region. In general the values in the *z/D=2* plane were larger than those in the *y/D=1* plane. The maximal absolute values of P^*, ω^* and Q^* were around 6, 10 and 11, respectively, in the *z/D=2* plane as shown in Figs. 1 and 2. The estimated uncertainties in the maximal values of P^*, ω^* and Q^* were 4, 4 and 14 percent, respectively.

6. SUMMARY

A technique is described for planar measurements of the mean rate-of-displacement tensor by using a conventional stereoscopic PIV system. The technique is tested in a turbulent jet in crossflow. Smoothness of the contour plots presented indicates the successful implementation of the technique. Consistency of the measurements is verified by the agreement between two sets of data obtained in two perpendicular planes. The estimated uncertainties in the maximal values of the vorticity magnitude (ω) and the production rate of turbulent kinetic energy (P) are 4 percent. Accuracy of the data can be improved and the dissipation rate of turbulent kinetic energy can be measured if optimal spacing between velocity vectors is employed. The feasibility of measuring the truncation error in the rotation– and strain–rate tensors is also demonstrated. Evaluation of the parameters in the Q–criterion and negative–λ_2 techniques helps to find locations of vortex cores in the mean flow field. Measurement uncertainties are discussed and algebraic relations for uncertainties in P and the parameter of the Q–criterion are presented.

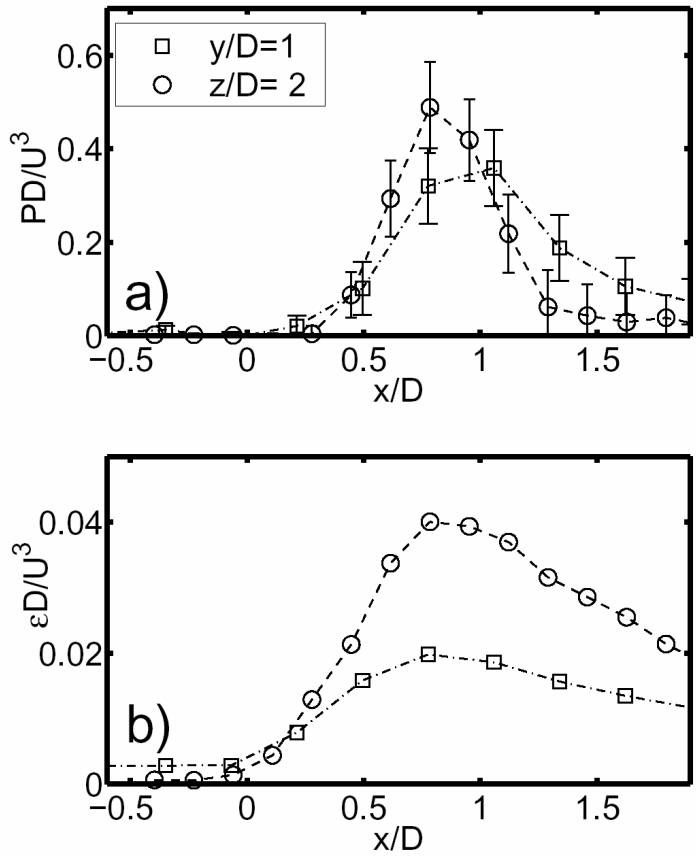

Fig. 8 Variations of the normalized rate of a) production of turbulent kinetic energy P^*, b) dissipation of turbulent kinetic energy ε^* at the intersection of the y/D=1 and z/D=2 planes.

ACKNOWLEDGMENTS

Thanks are due to Dr. Jakob M. Pedersen for his assistance in the PIV measurements. The first author acknowledges receipt of a grant between 1999 and 2001 in scope of the NATO Science Fellowship Programme by the Scientific and Technical Research Council of Turkey and also financial support from DTU, Department of Energy Engineering and Department of Mechanical Engineering.

REFERENCES

Andreopoulos, Y. and Honkan, A. (1996). "Experimental techniques for highly resolved measurements of rotation, strain and dissipation−rate tensors in turbulent flows", Measurement Science and Technology , 7, pp. 1462−1476

Antonia, A. and Mi, J. (1993). "Corrections for velocity and temperature derivatives in turbulent flows", Experiments in Fluids, 14, pp. 203−208

Benedict, L.H. and Gould, R.D. (1996). "Towards better uncertainty estimates for turbulence statistics", Experiments in Fluids, 22, pp. 129−136

Dahm, W.J.A., Su, L.K. and Southerland, K.B. (1992). "A scalar imaging velocimetry technique for fully−resolved four−dimensional vector velocity field measurements in turbulent flows", Physics of Fluids A, 4, pp. 2191−2206

Holman, J.P. (1978). "Experimental Methods for Engineers" , McGraw-Hill, New York, USA

Hu, H., Saga, T., Kobayashi, T., Taniguchi, N. and Yasuki, M. (2001). "Dual-plane stereoscopic particle image velocimetry: system set-up and its application on a lobed jet mixing flow", Experiments in Fluids, 31, pp. 277-293

Hunt, J.C.R., Wray, A.A. and Moin, P. (1988). "Eddies, stream and convergence zones in turbulent flows", Report CTR-S88, Center for Turbulence Research, NASA-Ames Research Center, Stanford University, California, USA

Jeong, J. and Hussain, F. (1995). "On the identification of a vortex", Journal of Fluid Mechanics, 285, pp. 69-94

Kawanabe, H., Kawasaki, K. and Shioji, M. (2001). "Evaluation of turbulence production and dissipation in a jet using high-resolution PIV", 4th International Symposium on Particle Image Velocimetry, Gottingen, Germany, September 17-19

Lim , T.T., New, T.H. and Luo, S.C. (2001). "On the development of large scale structures of a jet normal to a cross flow", Physics of Fluids, 13, pp. 770-775

Lourenco, L. and Krothapalli, A. (1995). "On the accuracy of velocity and vorticity measurements with PIV", Experiments in Fluids, 18, pp. 421-428

Meng, H. and Hussain, F. (1993). "In-line recording and off-axis viewing (IROV) technique for holographic particle velocimetry", Applied Optics, 34, pp. 1827-1840

Meyer, K.E., Özcan, O., Larsen, P.S., and Westergaard, C.H. (2001). "Stereoscopic PIV measurements in a jet in crossflow ", Second Int. Symp. on Turbulence and Shear Flow Phenomena, Stockholm, Sweden, June 27-29

Meyer, K.E., Özcan, O. and Westergaard, C.H. (2002). "Flow mapping of a jet in crossflow with stereoscopic PIV", Journal of Visualization, 5, pp. 225-231

Mullin, J.A and Dahm, W.J.A. (2004). "A study of velocity gradient fields at intermediate and small scales of turbulent shear flows via dual-plane stereo particle image velocimetry ", Report No: 044475-3, Laboratory for Turbulence and Combustion, University of Michigan, Ann Arbor, Michigan, USA

Nishino, K., Kasagi, N. and Hirata, M. (1989). "Three-dimensional particle tracking velocimetry based on automated digital image processing", Journal Fluids Engineering, 111, pp. 384-391

Özcan, O. and Larsen, P.S. (2003). "Laser Doppler anemometry study of a turbulent jet in crossflow ", AIAA Journal, 41, pp. 1614-1616

Pedersen, J.M. (2003). "Analysis of planar measurements of turbulent flows", Ph.D. Thesis, Dept. of Mechanical Eng., Technical University of Denmark, Lyngby, Denmark

Saarenrinne, P. and Piirto, M. (2000). "Turbulent kinetic energy dissipation rate estimation from PIV velocity vector fields", Experiments in Fluids, 29, pp. S300-S307

Tao, B. (2000). "Development of holographic particle image velocimetry and its application in three-dimensional velocity measurements and modeling of high Reynolds number flows", Ph.D. Thesis, Dept. of Mech. Eng., John Hopkins University, Baltimore, Maryland, USA

Tennekes, H. and Lumley, J.L. (1972). "A First Course in Turbulence", The MIT Press, Cambridge, Massachuhusetts and London, England

Wallace, J.M. and Foss, J. (1995). "The measurement of vorticity in turbulent flows", Annual Review of Fluid Mechanics, 27, pp. 469-514

Zhou, T., Zhou, Y., Yiu, M.W., and Chua, L.P. (2003). "Three-dimensional vorticity in a turbulent cylinder wake", Experiments in Fluids, 35, pp. 459-471